Liquid Crystals
Publication details, including instructions for authors and subscription information:
http://www.informaworld.com/smpp/title~content=t713926090

Transmission holographic polymer-dispersed liquid crystal based on fluorinated polymer matrices

Ju Yeon Woo[a]; Byung Kyu Kim[a]
[a] Department of Polymer Science and Engineering, Pusan National University, Busan 609-735, Korea

To cite this Article Woo, Ju Yeon and Kim, Byung Kyu(2008) 'Transmission holographic polymer-dispersed liquid crystal based on fluorinated polymer matrices', Liquid Crystals, 35: 8, 987 — 994
To link to this Article: DOI: 10.1080/02678290802308050
URL: http://dx.doi.org/10.1080/02678290802308050

Liquid Crystals,
Vol. 35, No. 8, August 2008, 987–994

Taylor & Francis
Taylor & Francis Group

Transmission holographic polymer-dispersed liquid crystal based on fluorinated polymer matrices

Ju Yeon Woo and Byung Kyu Kim*

Department of Polymer Science and Engineering, Pusan National University, Busan 609-735, Korea

(Received 18 April 2008; final form 27 June 2008)

The grating formation dynamics, morphology and electro-optical properties of transmission gratings of holographic polymer dispersed liquid crystals (HPDLCs) were investigated based on partial fluorination of the host polymer matrices by incorporating three different types of fluorinated monomer. Addition and increasing amounts of fluorinated monomer gave short saturation time and increased off-state diffraction efficiency with a maximum due to the chemical incompatibility between fluorinated compounds and LC, whereas the droplet size increased with increasing fluorinated monomer content. In addition, fluorinated monomer induced decreased switching voltage and increased response time due to the low anchoring energy at the polymer–LC interfaces and increased droplet size. At an optimum content of fluorinated monomer, a minimum switching voltage of $5\,V\,\mu m^{-1}$, a rise time of 0.25 ms and a decay time of 23.15 ms were obtained.

Keywords: holographic polymer-dispersed liquid crystal; polyurethane acrylate; fluorinated monomer; morphology; electro-optical properties

1. Introduction

As a new type of photoelectronic composite materials, holographic polymer-dispersed liquid crystals (HPDLCs) have shown great promise in a variety of applications such as optical components (*1*), flat panel displays (*2, 3*), lasers (*4*), information storage and many others (*5–8*).

HPDLC gratings are fabricated through holographic illumination of a homogeneous mixture of photoreactive monomer and liquid crystal (LC) by photopolymerisation-induced anisotropic phase separation (PIPS) (*9*). The periodic light intensity gradient resulting from holographic exposure induces mass transport of monomer into the regions of high light intensity and non-reactive LC into the dark regions (*10*). The morphology of HPDLCs consists of alternating layers of solid polymer and LC droplet-rich regions (*11*).

Some factors known to influence the overall properties of HPDLCs include LC droplet size and shape, amount of LC phase separation and refractive index mismatch of the polymer and LC (*12–15*). There have been numerous approaches to manipulate and improve HPDLC performance parameters such as diffraction efficiency, contrast, switching speed and voltages. These include photocurable acrylate systems (*1, 3, 6, 12, 14–18*), photopolymerisable thiol–ene based polymers (*9–11*, *19–20*), non-reactive surfactant-like molecules (*21–23*), conductive polymer molecules (*8, 24*), and so on (*25–28*). In most visibly recorded HPDLCs to date, a number of additives are typically required (*23*).

Previous publications reported enhanced phase separation of LCs, improved optical properties and more distinct morphologies with partial matrix fluorination (*29–31*). Despite the enhancements associated with the use of fluorinated monomer in holographic gratings, further improvement in electro-optical properties is still required. This report investigates the impact of polymerisation behaviour on LC phase separation, morphology and performance of HPDLCs made from fluorinated monomer-based polymerisations with a particular focus on perfluorinated materials. Both increasing extent of LC phase separation and decreasing anchoring strength by incorporating perfluorinated monomer yield high diffraction efficiency, well-defined grating morphology and low switching voltage. We measured real time and saturation diffraction efficiency, contact angle, scanning electron microscopy (SEM) images, anchoring strength, switching voltage and response time of the HPDLC films. Results may allow further optimisation of the performance of fluorinated monomer-based transmission HPDLC gratings.

2. Experimental

Materials

To synthesise the polyurethane acrylate (PUA) oligomers, molar excess of hexane diisocyanate (HDI) was reacted with bifunctional polypropylene glycol (PPG) (M_n=400 g mol^{-1}) to form isocyanate (NCO)-terminated polyurethane prepolymer, followed by capping with hydroxyehtyl acrylate (HEA). Detailed synthetic procedures are described elsewhere

*Corresponding author. Email: bkkim@pnu.edu

ISSN 0267-8292 print/ISSN 1366-5855 online

DOI: 10.1080/02678290802308050
http://www.informaworld.com

(*15, 32*). *N*-Vinylpyrrollidinone (NVP) and dipentaerythritol penta/hexaacrylate (DPHPA) were, respectively, used as mono- and multifunctional reactive diluents. NVP helps to dissolve different compounds in the mixture and reduces the viscosity, whereas DPHPA provides the mixture with high reactivity with polymers with a highly networked structure. The composition of oligomer/monofuctional/multifunctional diluents was fixed at 4/3/3 by weight.

Rose Bengal (RB, 0.3 wt%) was used as photoinitiator for holographic recording with an argon ion laser because it displays a broad absorption in the region of 450 to 560 nm and has a high triplet quantum yield (*33*). To this, 1.8 wt% of N-phenylglycine (NPG) was added as coinitiator. The excited RB undergoes an electron-transfer reaction in which NPG functions as an electron donor, producing an NPG radical. Free radical polymerisation is then initiated by the NPG radical (*5*).

Three types of fluorinated monomer, i.e. 1,1,1,3,3,3-hexafluoroisopropyl acrylate (HFIPA), 1H,1H,2H-perfluoro-1-hexene (PFH) and 1H,1H,2H,2H-perfluorodecyl acrylate (PFDA), were incorporated for partial fluorination of the host polymer ranging from 0, 10, 20 to 30 wt% (HFIPA20 is the HFIPA composition in prepolymer mixture). Figure 1 shows the chemical structures for the monomers used in this study.

In addition, 6 wt% of surfactant (octanoic acid) was added to the mixture to lower the switching field. E7 (BL001, Merck), a eutectic mixture of three cyanobiphenyl and one cyanoterphenyl mixture with high birefringence (n_o=1.5216, n_e=1.7462), adequate T_{NI} (61°C) and positive dielectric anisotropy ($\Delta\varepsilon$=13.8) was used as the LC at 35 wt%.

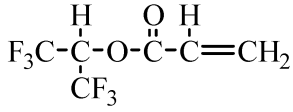

1,1,1,3,3,3-hexafluoroisopropyl acrylate (HFIPA)

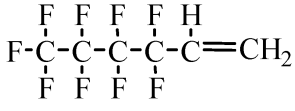

1H,1H,2H-perfluoro-1-hexene (PFH)

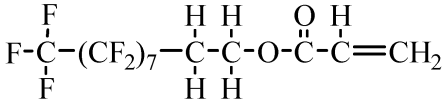

1H,1H,2H,2H-perfluorodecyl acrylate (PFDA)

Figure 1. Chemical structures of the fluorinated monomers used in the holographic system.

Grating fabrication and measurements

To fabricate the holographic grating, prepolymer/LC mixture was sandwiched between two indium tin oxide (ITO)-coated glass plates, with a gap of 10 μm, which was adjusted by a bead spacer. The writing geometry is accomplished by interference of two coherent laser beams (Ar ion laser) from a 514 nm of equal intensity with a total power of 100 mW cm^{-2} for 200 s. The intersection angle of the two beams outside the cell was fixed at 26°. The interference of the two beams established the periodic interference pattern according to Bragg's law ($\Lambda = \lambda/2\sin(\frac{\theta}{2})$, Λ=grating spacing, λ=wavelength of the writing beam).

The diffraction efficiencies of the holographic gratings were measured with a photodiode using an Ar ion laser. Diffraction efficiency was determined upon dividing the diffracted beam intensity of the sample cell by the transmitted beam intensity of blank cell. Real time grating formation was monitored using a He–Ne laser probe (633 nm) with incident angle set at the appropriate Bragg angle, since the material is not sensitive to red light. For electro-optical measurements, a square wave voltage (50 Hz sine wave pulse of 50 ms) operating from 0 to 80 V was applied across the HPDLC cell. The drive signal and the response of the photodiode were monitored with a digital storage oscilloscope (Hitachi VC-6023). The response time is defined as the time taken to relax from 90 to 10% of the maximum switching difference under an electric field. The grating morphology was visualised by scanning electron microscopy (SEM, Hitachi S430). For this, samples were prepared by freezing and fracturing the HPDLC cells in liquid nitrogen, and extracting the LC molecules in methanol for 24 h. The contact angle of the resin surface with a drop of LC was measured using a contact angle meter (Erma G-1).

3. Results and discussion

Miscibility and contact angle

The miscibility of a polymer and LC can be approximated by the solubility parameter (SP) gap. The SP is the square root of the cohesive energy density (E_c), which can be calculated by the group contribution theory (*34*). The SP of the LC used in this experiment was 20 (J cm^{-3})$^{1/2}$ and that of PUA is 22 on average,

whereas those with HFIPA, PFH, and PFDA are, respectively, 18.34, 12.35 and 15.08 $(J\,cm^{-3})^{1/2}$. The SP gap and hence the polymer–LC immiscibility increase according to PUA<HFIPA<PFDA<PFH.

The above results also agreed with contact angle measurements. Figure 2 shows contact angle as a function of fluorinated monomer content for various types of fluorinated monomer. Regardless of content of fluorinated monomer, contact angle is dramatically increased with the initial addition of fluorinated monomer, and further increases with an increasing amount of fluorinated monomer, which means an increase of immiscibility between the polymer matrix and LC. Among the fluorinated monomers, PFH, which has the lowest SP, exhibits the highest contact angle value. The rate and extent of polymer–LC phase separation should increase with increasing chemical immiscibility, which would give clean grating morphology and high diffraction efficiency.

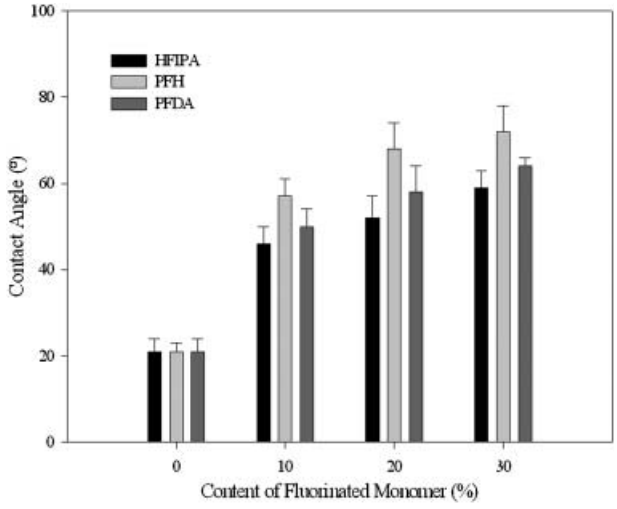

Figure 2. Contact angle as a function of fluorinated monomer content for various types of fluorinated monomer.

Grating formation dynamics

Figure 3 shows the real time diffraction efficiency as a function of irradiation time at various contents of fluorinated monomer. In the absence of fluorinated monomer, the diffraction efficiency does not show early overshoot and increases gradually to a saturation value due to the slow phase separation and diffusion leading to less vulnerable to droplet coalescence keeping the LC droplets small and uniform. With the addition and increasing content of fluorinated monomer (Figures 3(a) and 3(c)), the overshoot appears at a shorter irradiation time to give a higher saturation value, which is indicative of fast grating formation caused by easy diffusion and distinct separation due to the chemical incompatibility between fluorinated polymer matrix and LC. It can also be seen that PFH gives the fastest grating formation due to the large SP gap (Figure 3(b)). However, rapid migration of LC out of polymer layer following high content of fluorinated monomer would lead to extensive droplet coalescence to sizes larger than the critical one for scattering, giving rise to a decrease in diffraction efficiency, and this seems the case with HFIPA30, PFH20, PFH30 and PFDA30.

SEM morphology

The performance of holographic gratings in terms of diffraction efficiency, switching voltage, speeds and background scatter is inherently related to the solid-state morphology of the grating structures (*6*). Figure 4 shows a SEM image of the HPDLC grating as a function of type of fluorinated monomer. The dark regions represent the original location of the LC droplets and the bright regions represent networked polymer matrix. The grating period calculated according to Bragg's law was 1267 nm. However, due to the shrinkage upon polymerisation, an important issue of a number of recent works (*15*), the fabricated grating spacing is about 1100 nm. Grating images of HFIPA, PFH and PFDA are fairly well fabricated and droplet size increases according to HFIPA<PFDA<PFH, an order that agrees with increasing SP gap (immiscibility) measurements. Specifically, histogram analyses of the SEM image read 120–180 nm for PFDA20 and 140–210 nm for PFH20.

Figure 5 shows the morphology of the HPDLC grating as a function of fluorinated monomer (PFH) content. The average size of LC domains formed with PFH (150–200 nm) is larger than the one formed without PFH (60–100 nm). With increasing content of PFH, enhanced phase separation caused by the increased immiscibility between fluorinated polymer matrix and LC gave large LC channels with marginally increased droplet size, leading to the high diffraction efficiency, which in other words is due to a large mismatch in refractive index between polymer and LC phases.

Diffraction efficiency

Figure 6 shows the diffraction efficiency as a function of fluorinated monomer content for various types of fluorinated monomer. With the addition of fluorinated monomer, diffraction efficiency initially increases and reaches a maximum of over 90% with HFIPA20, PFH10 and PFDA20. This implies that the good diffusion and enhanced LC phase separation cause large LC channels leading to the highest diffraction

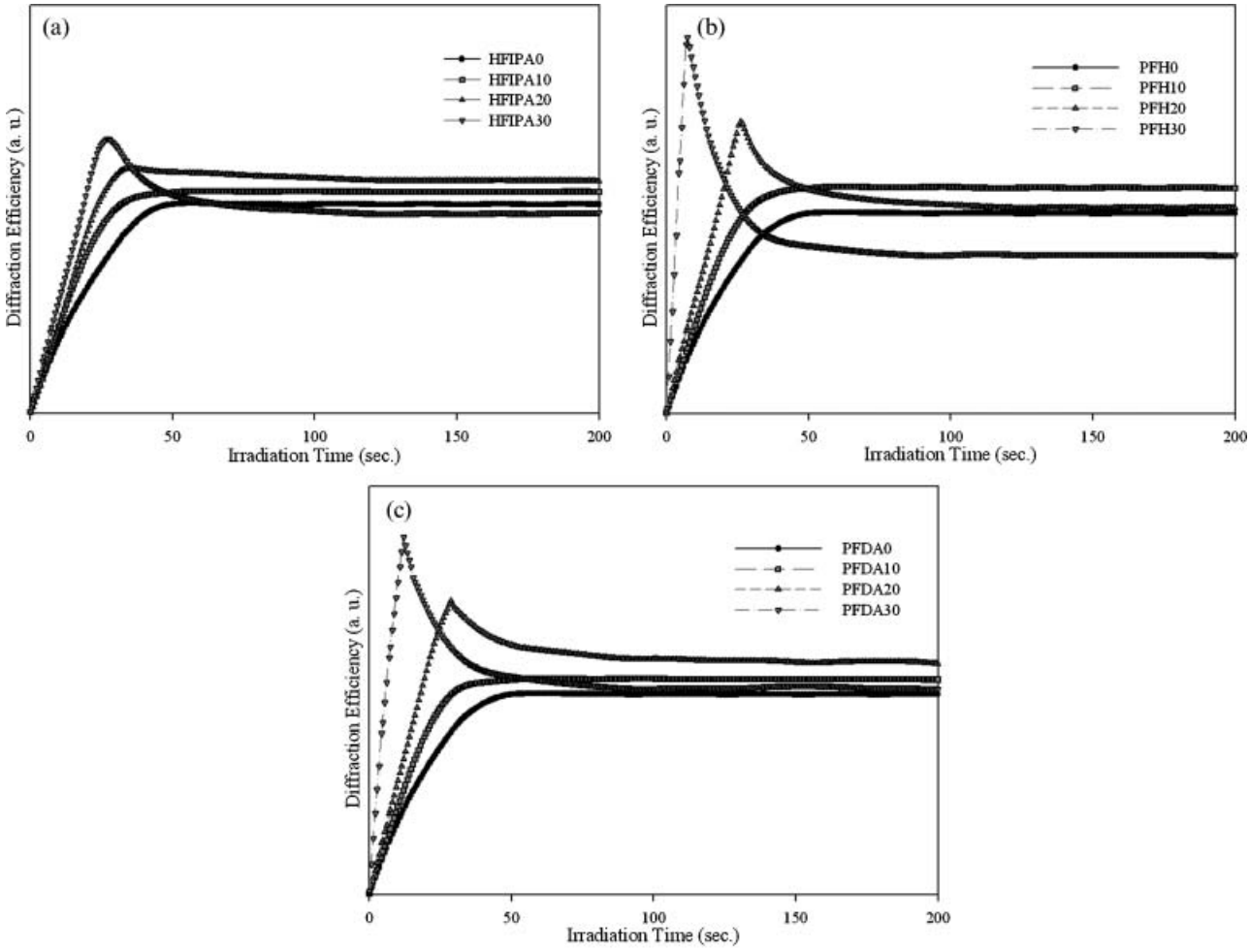

Figure 3. Real-time diffraction efficiency as a function of irradiation time at various contents of fluorinated monomer in a developing HPDLC grating prepared with HFIPA (a), PFH (b) and PFDA (c) (irradiated at 633 nm).

efficiency due to a large difference in refractive index between polymer and LC caused by the increased immiscibility between fluorinated polymer matrix and LC, as noted from the SEM morphology. However, beyond the maximum content, diffraction efficiency slightly decreases. This seems reasonable since high content of fluorinated monomer causes rapid migration of LC molecules into the LC-rich phase, which leads to extensive coalescence to form large LC droplets. This lowers droplet density and enlarges LC domain size leading to high scattering loss.

Electro-optical properties

Figure 7 shows the diffraction efficiency of the film as a function of applied voltage for various contents of fluorinated monomer. Switching voltage is defined as the voltage at a 90% drop in diffraction efficiency. Upon applying voltage, diffraction efficiency decreases implying that LC molecules are oriented along the electric field direction and light is transmitted. Regardless of type of fluorinated monomer, when a voltage is applied across the film, diffraction efficiency decreases with increasing content of fluorinated monomer due to the significant increase in the droplet size and distribution of nematic domains.

For the HPDLC systems, the anchoring strength plays a very important role in dictating the electro-optical properties. Threshold voltage (E_{th}) and surface anchoring strength (W_s) are related by the following equation (*30, 35*)

$$E_{th}^2 = \frac{8\pi W_s(\varepsilon_{//} + 2\varepsilon_P)(\varepsilon_\perp + 2\varepsilon_P)}{3R\varepsilon_o\varepsilon_P^2(\varepsilon_{//} - \varepsilon_\perp)}, \qquad (1)$$

where ε_o, ε_P, $\varepsilon_{//}$, $\varepsilon_\perp$ and R are, respectively, the vacuum permittivity, dielectric constant of polymer, the dielectric constants parallel and perpendicular to nematic director of the LC and average radius of LC. In our experiment, ε_o, ε_P, $\varepsilon_{//}$, $\varepsilon_\perp$ are 8.85×10^{-12}, 3,

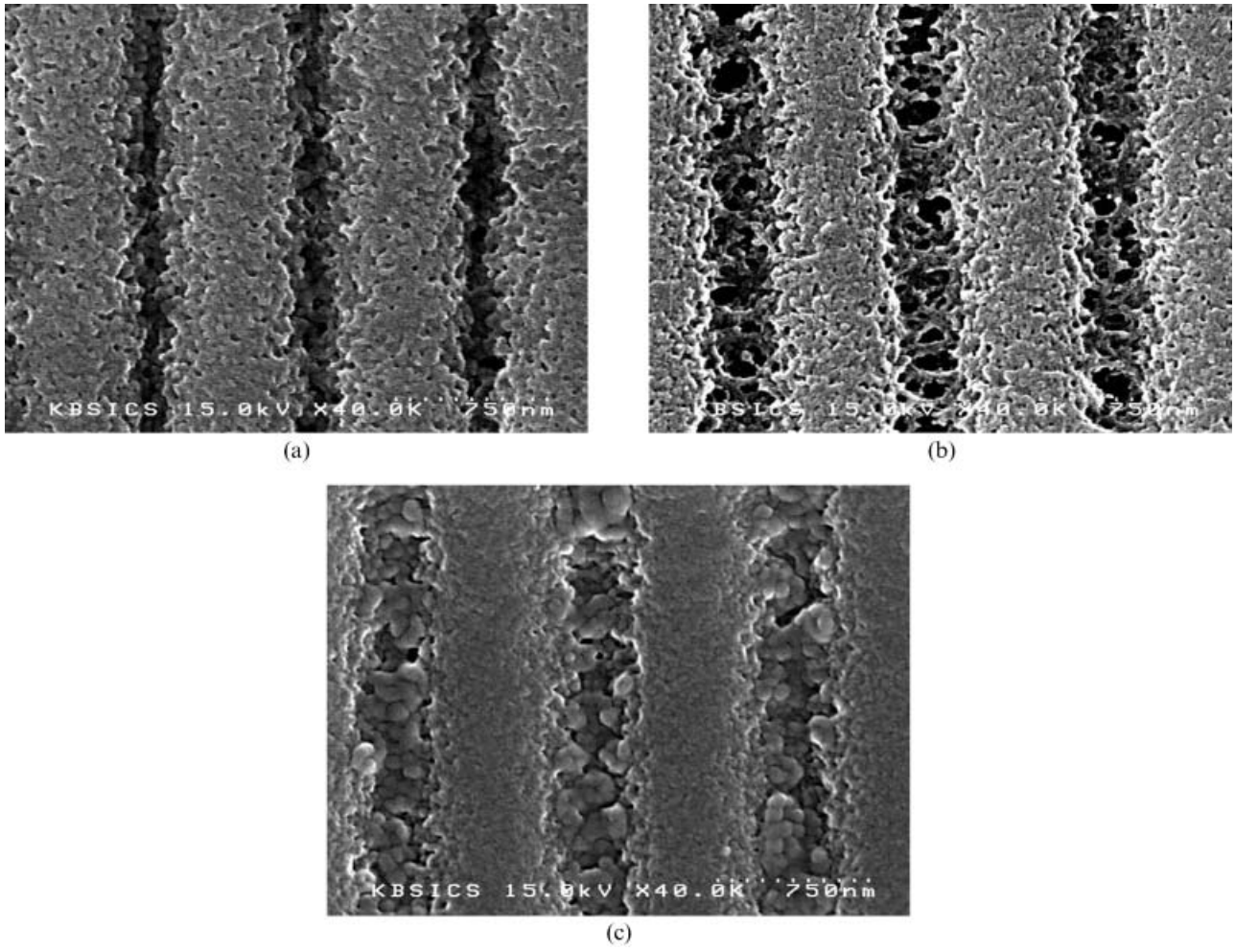

Figure 4. SEM image of the transmission gratings prepared with HFIPA20 (a), PFH20 (b) and PFDA20 (c).

19.0 and 5.4, respectively. The R and E_{th} are obtained from SEM morphology and Figure 7, respectively. Anchoring strengths (W_s) calculated from the Equation (1) increase in the order HFIPA<PFDA< PFH.

Figure 8 shows the anchoring strength as a function of PFH content. It can be seen that with increasing content of PFH the anchoring strength decreases. For PFH30, which has the lowest anchoring strength, the switching voltage is about $4\,V\,\mu m^{-1}$ and diffraction efficiency is close to zero due to the more perfect orientation of the LC molecules.

Figure 9 shows rise time and decay time of HPDLC films for various applied voltage; the detailed data at saturation voltage are given in Table 1. Rise time is expected to be field dependent and rapidly decreases with increasing voltages and is less than 1 ms at saturation voltage. On the other hand, decay time shows the opposite tendency to the rise time, i.e. decay time increases with increasing voltage and is approximately 23 ms. A slow decay of an internal electric field caused by the migration of ions in the film could explain the increase of decay time with increasing field (*7*). Regardless of type of fluorinated monomer, rise time and decay time slightly increase with the addition and increasing content of fluorinated monomer. It is well known that the response time depends on the surface anchoring energy, elastic free energy and viscosity, as well as the LC droplet size. The decrease of anchoring strength and the increase of LC droplet size with fluorinated monomer both account for the increase in response time.

4. Conclusions

Fluorination of the host polymer matrices by incorporating three different types of fluorinated monomer based on the poor solubility and low anchoring energy have been introduced to the formulation of holographic polymer-dispersed liquid crystal, and the effects have been studied in terms of contact angle,

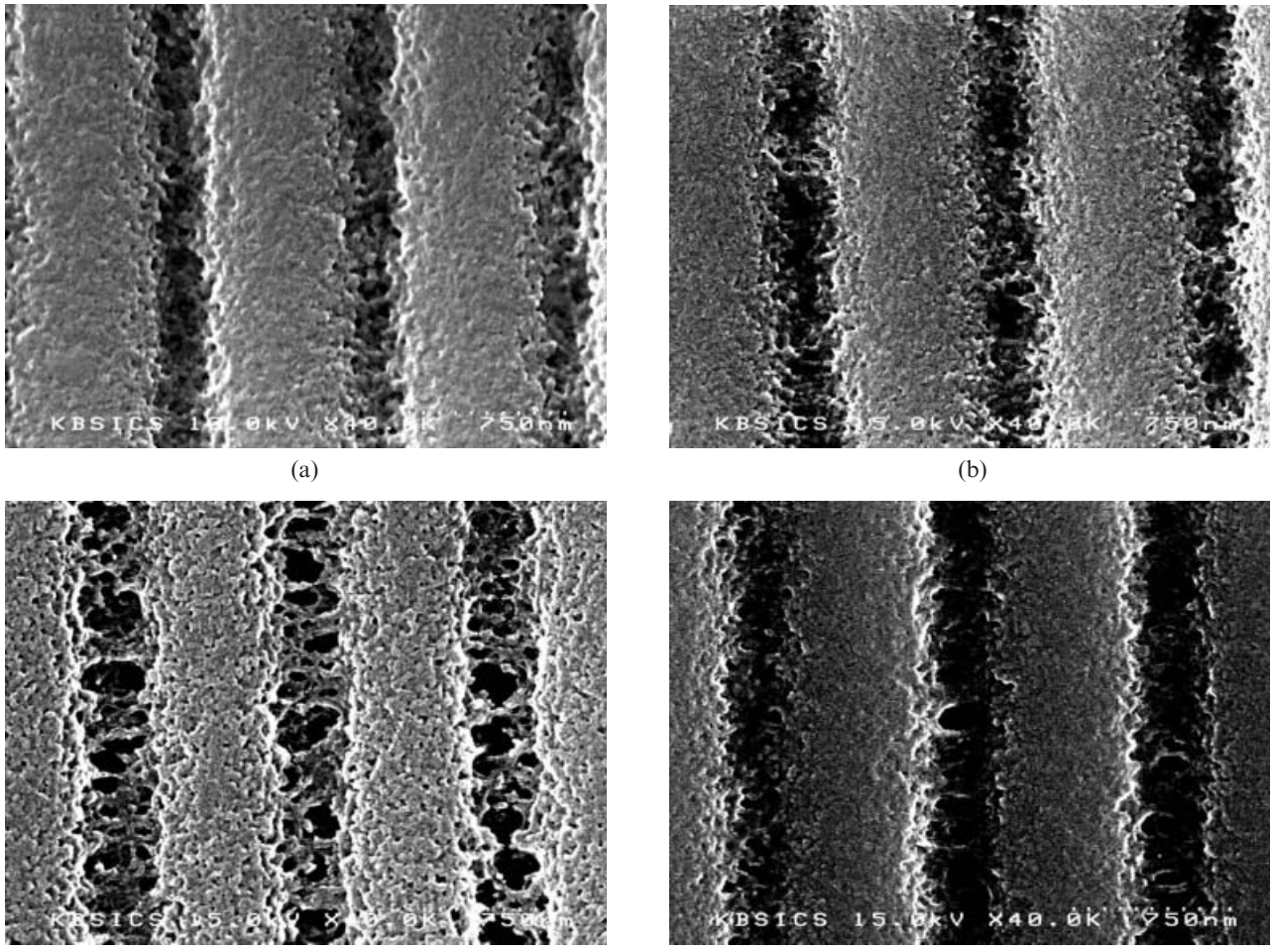

Figure 5. SEM image of the transmission gratings prepared with PFH0 (a), PFH10 (b), PFH20 (c) and PFH30 (d).

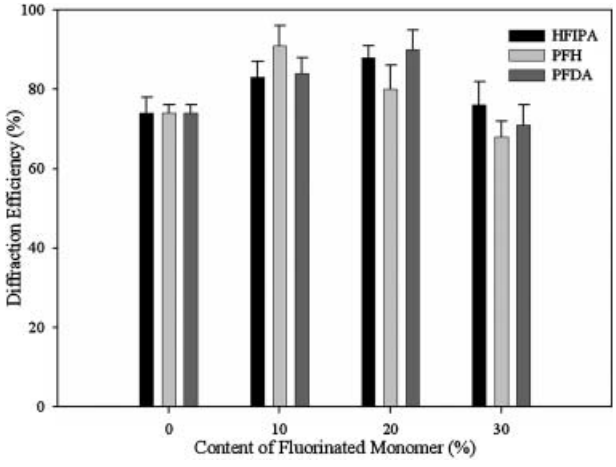

Figure 6. Diffraction efficiency as a function of fluorinated monomer content for various types of fluorinated monomer.

grating formation dynamics, morphology, diffraction efficiency and electro-optical properties of the films.

Addition of fluorinated monomer to polymer directly reduced the miscibility between polymer matrix and LC, giving rise to great phase separation, large LC channel and great mismatch of refractive index, and eventually high diffraction efficiency of the composite film at a particular composition (HFIPA20, PFH10 and PFDA20). However, beyond the maximum concentration, subsequent phase separation becomes fast due to the great immiscibility, which leads to extensive coalescence to form large LC droplets leading to high scattering loss (HFIPA30, PFH20, PFH30 and PFDA30).

Driving voltage decreased with the addition of fluorinated monomer since it helps the orientation of LC molecule with its low surface energy and increased droplet size. Anchoring strength and driving voltage of perfluorinated monomers (PFH

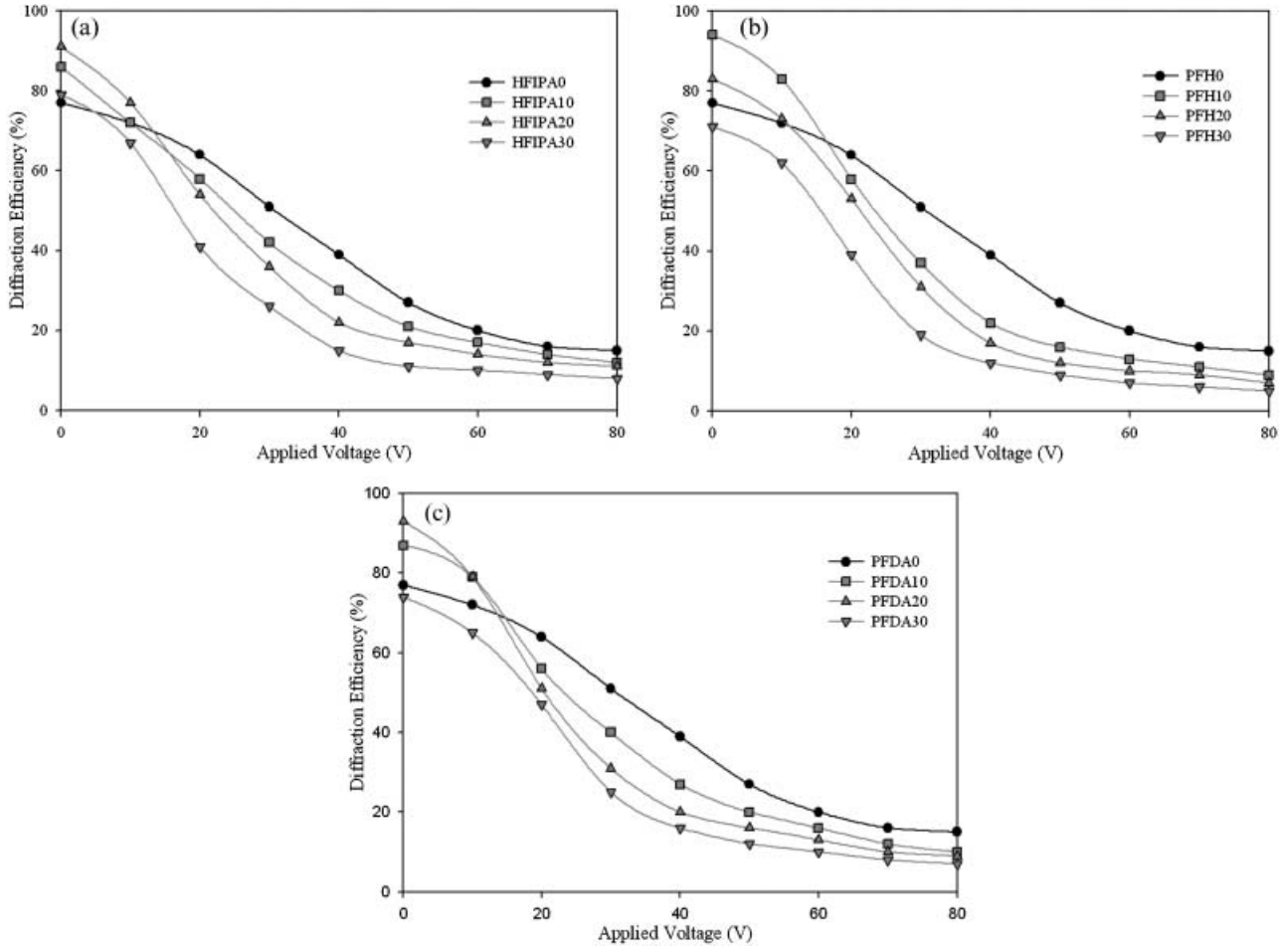

Figure 7. Diffraction efficiency as a function of applied voltage at various contents of fluorinated monomer of HPDLC films prepared with HFIPA (a), PFH (b) and PFDA (c).

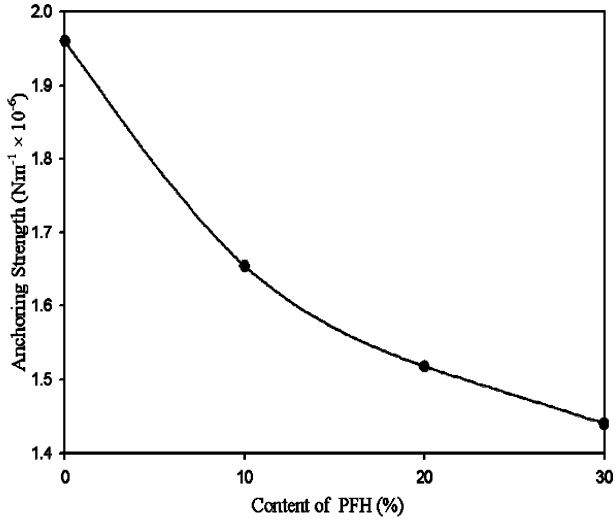

Figure 8. Anchoring strength as a function of content of PFH.

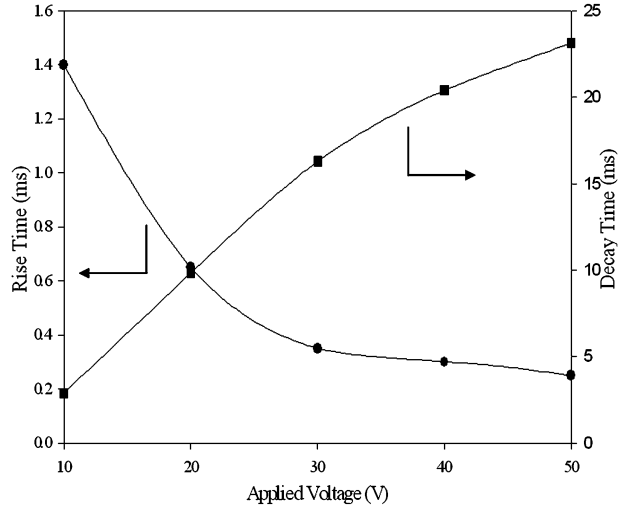

Figure 9. Rise time and decay time of HPDLC films as a function of applied voltage (PFH10).

Table 1. Response time of the film as a function of fluorinated monomer content for various types of fluorinated monomer ($5\,V\,\mu m^{-1}$).

Response time /ms	Type of fluorinated monomer	Content of fluorinated monomer /% 0	10	20	30
Rise time	HFIPA	0.20	0.20	0.25	0.25
	PFH	0.20	0.25	0.30	0.35
	PFDA	0.20	0.25	0.30	0.30
Decay time	HFIPA	18.45	20.30	21.45	21.90
	PFH	18.45	23.15	25.40	27.25
	PFDA	18.45	22.70	23.55	24.10

and PFDA) were lower than that of HFIPA due to the relatively low SP leading to large droplet size. On the other hand, rise time and decay time increased with the addition and increasing content of fluorinate monomer due to the low anchoring energy and increased droplet size. An optimum type and content of fluorinated monomer was obtained with PFH10, where a minimum switching voltage of $5\,V\,\mu m^{-1}$, rise time of 0.25 ms, a decay time of 23.15 ms and diffraction efficiency over 90% were obtained.

Acknowledgements

The research was supported by the NCRC Organized at DNU (Grant No. R15-2006-022-01001).

References

(1) Domash L.; Crawford G.; Ashmead A.; Smith R.; Popovich M.; Storey J. *SPIE Proc.* **2000**, *4107*, 46–58.
(2) Kato K.; Hisaki T.; Date M. *Jap. J. Appl. Phys.* **1999**, *38*, 1466–1469.
(3) Sutherland R.L.; Natarajan L.V.; Tondiglia V.P.; Bunning T.J. *SPIE Proc.* **2003**, *5216*, 34–43.
(4) Jakubiak R.; Bunning T.J.; Vaia R.A.; Natarajan L.V.; Tondiglia V.P. *Adv. Mater.* **2003**, *15*, 241–244.
(5) Qi J.; Crawford G.P. *Display* **2004**, *25*, 177–186.
(6) Pogue R.T.; Sutherland R.L.; Schmitt M.G.; Natarajan L.V.; Siwecki S.A.; Tondiglia V.P.; Bunning T.J. *Appl. Spectrosc.* **2000**, *54*, 12A–28A.
(7) Nalwa H.S. *Handbook of Advanced Electronic and Photonic Materials and Devices*; Academic Press: San Diego, 2001.
(8) Nicoletta F.P.; Chidichimo G.; Cupelli D.; Filpo G.D.; Benedittis M.D.; Gabriele B.; Salerno G.; Fazio A. *Adv. Funct. Mater.* **2005**, *15*, 995–999.
(9) Senyurt A.F.; Warren G.; Whitehead J.B. Jr.; Hoyle C.E. *Polymer* **2006**, *47*, 2741–2749.
(10) White T.J.; Natarajan L.V.; Tondiglia V.P.; Lloyd P.F.; Bunning T.J.; Guymon C.A. *Polymer* **2007**, *48*, 5979–5987.
(11) White T.J.; Natarajan L.V.; Tondiglia V.P.; Lloyd P.F.; Bunning T.J.; Guymon C.A. *Macromolecules* **2007**, *40*, 1121–1127.
(12) Woo J.Y.; Kim E.H.; Kim B.K. *ChemPhysChem* **2008**, *9*, 141–146.
(13) Beev K.; Criante L.; Lucchetta D.E.; Simoni F.; Sainov S. *Opt. Commun.* **2006**, *260*, 192–195.
(14) He J.; Yan B.; Yu B.; Wang S.; Zeng Y.; Wang Y. *Eur. Polym. J.* **2007**, *43*, 2745–2749.
(15) Kim E.H.; Woo J.Y.; Kim B.K. *Macromol. Rapid Commun.* **2006**, *27*, 553–557.
(16) Olenik I.D.; Jazbinsek M.; Sousa M.E.; Fontecchio A.K.; Crawford G.P.; Copic M. *Phys. Rev. E* **2004**, *69*, 051703–051710.
(17) Sarkar M.D.; Gill N.L.; Whitehead J.B.; Crawford G.P. *Macromolecules* **2003**, *36*, 630–638.
(18) White T.J.; Guymon C.A. *Polym. Mater. Sci. Engng* **2003**, *89*, 452–453.
(19) Natarajan L.V.; Shepherd C.K.; Brandelik D.M.; Sutherland R.L.; Chandra S.; Tondiglia V.P.; Tomlin D.W.; Bunning T.J. *Chem. Mater.* **2003**, *15*, 2477–2484.
(20) Cramer N.B.; Bowman C.N. *J. Polym. Chem. A* **2001**, *39*, 3311–3319.
(21) Woo J.Y.; Kim B.K. *ChemPhysChem* **2007**, *8*, 175–180.
(22) Klosterman J.; Natarajan L.V.; Tondiglia V.P.; Sutherland R.L.; White T.J.; Guymon C.A.; Bunning T.J. *Polymer* **2004**, *45*, 7213–7218.
(23) Liu Y.J.; Sun X.W.; Dai H.T.; Liu J.H.; Xu K.S. *Opt. Mater.* **2005**, *27*, 1451–1455.
(24) Cupelli D.; Nicoletta F.P.; Filpo G.D.; Chidichimo G.; Fazio A.; Gabriele B.; Salerno G. *Appl. Phys. Lett.* **2004**, *85*, 3292–3294.
(25) Woo J.Y.; Kim E.H.; Kim B.K.; Cho Y.H. *Liq. Cryst.* **2007**, *34*, 527–533.
(26) Li W.; Zhang H.; Wang L.; Ouyang C.; Ding X.; Cao H.; Yang H. *J. Appl. Polym. Sci.* **2007**, *105*, 2185–2189.
(27) Cho Y.H.; He M.; Kim B.K.; Kawakami Y. *Sci. Technol. Adv. Mater.* **2004**, *5*, 319–323.
(28) Bunning T.J.; Natarajan L.V.; Tondiglia V.P.; Sutherland R.L. *Annu. Rev. Mater. Sci.* **2000**, *30*, 83–115.
(29) Schulte M.D.; Clarson S.J.; Natarajan L.V.; Tomlin D.W.; Bunning T.J. *Liq. Cryst.* **2000**, *27*, 467–475.
(30) Sarkar M.D.; Qi J.; Crawford G.P. *Polymer* **2002**, *43*, 7335–7344.
(31) Jung J.A.; Kim B.K. *Opt. Commun.* **2005**, *247*, 125–132.
(32) Woo J.Y.; Kim E.H.; Yoon T.H.; Kim J.C.; Kim B.K. *Liq. Cryst.* **2007**, *34*, 1115–1120.
(33) Drzaic P.S. *Liquid Crystal Dispersions*; World Scientific: Singapore, 1995.
(34) Brandrup J.; Immergut E.H.; Grulke E.A. *Polymer Handbook*; John Wiley & Sons: New York, 1999.
(35) Levy O. *Phys. Rev. Lett.* **2001**, *86*, 2822–2825.